Applied Catalysis B: Environmental 165 (2015) 260–268

Contents lists available at ScienceDirect

Applied Catalysis B: Environmental

journal homepage: www.elsevier.com/locate/apcatb

Study of the effects of surface modification by thermal shock method on photocatalytic activity of TiO_2 P25

Tien Khoa Le[a], Delphine Flahaut[b], Hervé Martinez[b], Huu Khanh Hung Nguyen[a], Thi Kieu Xuan Huynh[a,*]

[a] University of Science, Vietnam National University - Ho Chi Minh City, 227 Nguyen Van Cu Street, Ho Chi Minh City, Vietnam
[b] IPREM/ECP (UMR 5254), University of Pau, Hélioparc, 2 av. Pierre Angot, 64053 Pau cedex 9, France

ARTICLE INFO

Article history:
Received 24 May 2014
Received in revised form 6 October 2014
Accepted 8 October 2014
Available online 17 October 2014

Keywords:
TiO_2
Thermal shock
Adsorption behavior
Surface properties
Photocatalytic activity

ABSTRACT

In this study, we have modified TiO_2 P25 photocatalyst by thermal shock method at different temperatures in order to study the effects of thermal shock process on the crystal structure, surface properties and photocatalytic activity. The thermal-shock-modified catalysts were respectively characterized by X ray diffraction (XRD), scanning electronic microscopy (SEM), X ray photoelectron spectroscopy (XPS) and UV–vis diffuse reflectance spectra and compared with thermal-shock-fluorinated TiO_2 catalysts. The photocatalytic activity was evaluated via the degradation of methylene blue under UV and visible light irradiation. The results show that the deficiency of oxygen on the surface of catalysts created by thermal shock at 500 °C can enhance the photocatalysis under both UV and visible light. Moreover, when the thermal shock was combined with the fluorination of TiO_2, the photocatalytic performance was further improved. However, the thermal shock from 700 °C promoted the growth of particles and the phase transition from anatase to rutile, which resulted in two different effects: inhibit the photocatalysis under UV irradiation but improve it under visible irradiation.

1. Introduction

During the past decade, a great deal of effort has been devoted to improve the photocatalytic activity of TiO_2 by doping this oxide with transition metals or non metal ions. It was generally observerd that the presence of these dopants on substituted or interstitial sites of TiO_2 lattice could induce the formation of defects on the surface and in the bulk of TiO_2 such as dislocation defect, oxygen vacancies and titanium vacancies. However, the effect of these defects on the photocatalytic activity is still under debate. Some studies demonstrated that the defects can increase the photocatalytic performance and extend it into the visible light region [1–5] whereas the others found a decrease of TiO_2 activity with the increase of defects [6–8]. It should be noted that there always exist structural defects on the surface and inside TiO_2 bulk [9]. The defects formed in the bulk might lower its activity since they provide sites for the recombination of photogenerated charge carriers, while the presence of defects on the surface of semiconductors is beneficial for the photocatalysis [1,6,10,11]. The surface defects may act as electron capture centers, retarding the recombination of charge carriers [12,13]. Moreover, the surface oxygen vacancies can promote the adsorption of O_2 molecules [14,15], which can capture photogenerated electrons to produce high oxidative species such as O_2^- radical groups. Therefore, introducing defects on the surface of photocatalysts can be a feasible way to improve the photocatalytic activity.

In our previous studies, fluorinated TiO_2 was successfully prepared by a simple thermal shock method [16,17]. This is the method which allowed us to carry out solid phase reactions at high temperatures during a short time. The results showed that the fluorination by thermal shock method in determined conditions could only affect the surface of TiO_2 without modifying the bulk structure and the morphology. Although TiO_2 fluorination was carried out by many previous study which indicated that the surface fluorination or insertion of F atoms into TiO_2 lattice only improve the UV light induced photocatalytic activity, our fluorinated catalysts demonstrated better activities under both UV and visible light illumination than naked TiO_2 P25 due to the formation of surface adsorbed fluoride ions and surface defects. This result indicated that the effect of thermal shock process play a very important role in photocatalytic activity of TiO_2.

However, the role of thermal shock method without fluorination in the photocatalytic performance of TiO_2 was not elucidated. R.G. Nair et al. [18] studied the influence of thermal treatment at various temperatures, from 600 to 850 °C during 1 h on the properties

* Corresponding author. Tel.: +84 8 38 30 21 46; fax: +84 8 38 35 00 96.
E-mail address: htkxuan@hcmus.edu.vn (T.K. Xuan Huynh).

http://dx.doi.org/10.1016/j.apcatb.2014.10.024
0926-3373/

of TiO_2 but the thermal treatment used in their study is totally different from our thermal shock method. Therefore, in this work, we investigated the effects of thermal shock process at different temperatures on crystal structure, particle size, surface composition and then evaluated the photocatalytic activity of modified catalysts under both UV and visible light irradiation. Then the properties of modified TiO_2 by thermal shock method were compared with that of fluorinated TiO_2 to study the synergic effects of thermal shock and fluorination process. It should be noted that the photocatalytic tests for fluorinated TiO_2 catalysts in [16] was only carried out under visible light. Thus we also evaluated their photocatalytic performance under UV irradiation for a better overall comparison with thermal shock modified TiO_2 in this work.

2. Experimental

2.1. Thermal shock process

TiO_2 P25 (Evonik Aeroxide), a mixture of anatase and rutile with a primary particle size of 20–50 nm, was used as the target catalyst to modify by thermal shock method because it is so far the best commercial photocatalyst. TiO_2 was washed and dried at 150 °C. Then this powder was placed in an alumina crucible and rapidly put into a furnace for thermal shock (TS) sequences of 5 min at different temperatures: 500, 700, 950 °C and at normal atmospheric pressure. After 5 min, the samples were directly removed from the furnace, cooled down to the room temperature and grounded to obtain the final powder products. These samples were labeled as P25-X (with X the TS temperature).

For comparison, fluorinated TiO_2 samples were also prepared by TS method as described in our previous study [16]. Briefly, TiO_2 P25 nanoparticles were suspended in 10 mL of a KF solution (0.625 mol L^{-1}) with the molar ratio of fluorine to titanium of 1:1. The obtained white suspension was dried at 150 °C for 3 h and underwent a TS process at 500, 700 and 950 °C during 5 min. These fluorinated samples were labeled as FTO-X (with *X* the temperature of thermal shock process).

2.2. Characterization

The powder X ray diffraction (XRD) patterns of catalysts were measured on a SIEMENS D5000 X ray diffractometer using Cu Kα radiation (λ = 1.5406 Å) in order to investigate the crystal structure and phase composition. The acceleration voltage and the applied current were 40 kV and 20 mA, respectively. Data was collected from 20° to 80° (2θ) with a scan rate of 0.03° 2θ s^{-1}. The Rietveld refinement was carried out using the Fullprof 2009 structure refinement software [19].

Scanning electron microscopy (SEM) images were taken using a scanning electron microscope Hitachi S-4800 operating at the accelerating voltage of 30 keV and the probe current of 10^{-10} A. The surface area was measured by N_2 adsorption at 77 K using a Quantachrome NOVA 1000 Surface Area and Pore Size Analyzer. A five-point nitrogen adsorption isotherm was used to determine the BET surface area of catalysts.

The surface atomic composition and the chemical environment of elements on sample surface were analyzed by X ray photoelectron spectra (XPS) obtained on a Thermo K-alpha system with a hemispherical analyzer and a microfocused (analysis area was ca. 200 μm^2) monochromatized radiation Al Kα (1486.6 eV) operating at 75 W under the residual pressure of 1×10^{-7} mBar. Surface charging was minimized by a neutralizer gun, which sprays the low energy electrons and Ar^+ ions over the sample surface. All the binding energy values are calibrated by using the standard binding energy of contamination carbon (C 1s = 285.0 eV) as a reference. The treatment of core peaks was carried out using a nonlinear Shirley-type background [20]. The quantification of surface composition was based on Scofield's relative sensitivity factors [21].

UV–vis absorption spectra of catalysts were obtained using a UV–vis spectrophotometer with an integrating sphere (JASCO V-550). They were recorded at room temperature in steps of 2 nm, in the range 200–900 nm with a bandwidth of 2 nm and were referenced to $BaSO_4$. The band gap energy E_g can be evaluated from a plot of $(\alpha)^{1/2}$ versus photon energy ($h\upsilon$) where α is the absorption coefficient [22].

2.3. Photocatalytic study

The photocatalytic activities of TiO_2 P25 and modified samples by TS method as well as fluorinated samples were evaluated through the degradation of methylene blue (MB). The tests were performed in a reactor which consists of a glass beaker containing 250 mL of aqueous MB solution (10^{-5} mol L^{-1}) with catalyst (0.5 g L^{-1}), cooled by continuous water flow and stirred continuously by magnetic agitator in the dark for 30 min to ensure the adsorption/desorption equilibrium. The reaction solution was then irradiated by an 8-W UV light lamp (350 nm) or an 8-W visible light lamp (420 nm) placed about 15 cm above the solution surface. The initial pH of prepared suspensions was seven and did not considerably change during all the experiments (pH = 6.8 ± 0.2). During the illumination, 10 mL of dispersions were sampled every 30 min, centrifuged and analyzed by SP-300 Optima spectrophotometer.

3. Results and discussions

3.1. Crystal structure and morphology

X ray diffraction was used to investigate the effect of TS process on the crystal structure and phase composition of TiO_2 P25. Fig. 1 shows the X ray diffractograms of TiO_2 P25 and TS-modified catalysts at different temperatures. The phase composition of these samples was summarized and compared with those of fluorinated catalysts obtained in our previous study [16] in Table 1. TiO_2 P25 consists of a mixed phase of anatase (space group $I4_1/amd$, JCPDS No. 21-1272) and rutile (space group $P4_2/mnm$, JCPDS No. 21-1276) in the ratio of 90:10. When TiO_2 P25 was modified with TS process at 500 °C, no modification of phase composition was observed. The width of peaks of P25-500 sample also remains unchanged in comparison with TiO_2 P25. This is similar to XRD results of FTO-500 sample, indicating that the TS process at this temperature does not change the phase composition and the oxide crystallite size. However, when TS temperature reaches at 700 °C, the rutile amount slightly increases (about 15%) whereas the anatase amount decreases (about 85%). This is in good agreement with the phase transition from anatase to rutile which generally occurs at 700 °C [23]. At TS temperature of 950 °C, XRD pattern shows that all anatase phase was completely transformed into rutile phase. The average diameter of anatase and rutile crystallites were respectively calculated from the full width of half maximum (FWHM) of diffraction peaks by using the Debye–Scherrer formula:

$$D_{hkl} = \frac{k\lambda}{\beta \cos\theta}$$

where D_{hkl} is the crystallite size, k is the constant dependent on crystallite shape (0.9), λ is the wavelength of copper Kα X-ray radiation (1.5406 Å), β is the FWHM of the most intense diffraction lines for anatase (1 0 1) and rutile (1 1 0) and θ is their diffraction angle (Table 1). The crystallite sizes are found to be in nanoscale and about 20–50 nm for both anatase and rutile phases in TiO_2 P25, PTO-500 and PTO-700 samples. The average rutile crystallite size only increased to 69.5 nm when TiO_2 P25 was TS-modified at 950 °C.

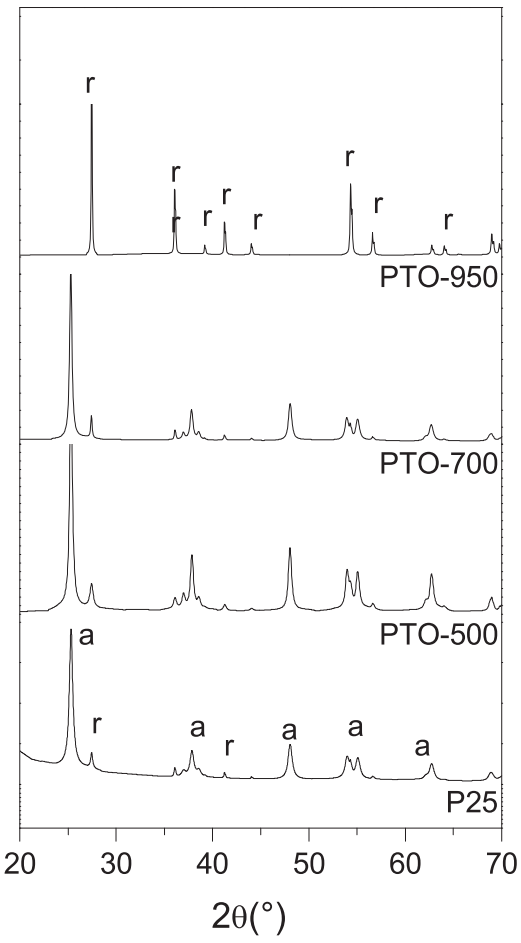

Fig. 1. XRD patterns of TiO_2 P25 and TS-modified samples (a and r represent the anatase and rutile phases, respectively).

On the other hand, when TiO_2 was modified with KF by TS method at 700 and 950 °C, beside the slight increase of rutile crystallite size, a new phase, $K_2Ti_6O_{13}$ was observed (space group C2/m, JCPDS No. 73-1398) in their diffractograms [16]. The results suggested that the TS method at high temperatures did not only result in the phase transition and the crystallite size increase of TiO_2 but also promoted the solid phase reaction between KF and TiO_2.

The morphology and particle size of catalysts were studied by SEM. The SEM image of TiO_2 P25 (Fig. 2a) presents sphere-like particles in an agglomerated status with a homogeneous size of 20–50 nm. The shape and size of these particles were not modified with TS process at 500 °C (Fig. 2b) and 700 °C (Fig. 2c). However, when the TS process was carried out at 950 °C, the particle size was strongly modified. Fig. 2d shows the sphere-like particles of P25-950 sample with the size of 100–250 nm. The results were quite different from the particle size evolution observed for FTO sample in [16]. When TiO_2 P25 was fluorinated at TS of 500 °C, the particle shape and size were almost identical to those of naked TiO_2 P25. But above 700 °C, the rod-like particles appeared and grown with TS temperature, which is consistent with the formation of $K_2Ti_6O_{13}$ phase.

The BET surface areas of TiO_2 P25, TS-modified and TS-fluorinated samples are listed in Table 1. For TS-modified TiO_2 catalysts, the BET values are in a good agreement with the microscopic characteristics. The PTO-500 shows a surface area of 34.8 $m^2\,g^{-1}$, which is identical to TiO_2 P25, whereas the PTO-700 shows a reduced surface area (26.6 $m^2\,g^{-1}$) due to the increase of particle size. Surprisingly, when TiO_2 was TS-fluorinated at 500 °C, the BET surface area was found to be 47.8 $m^2\,g^{-1}$, indicating that the fluorination can increase the surface area.

3.2. Surface characterization

The surface composition and the chemical environments of C, O, Ti elements on the surface of TiO_2 P25 and TS-modified catalysts were investigated by XPS. All the results were reported in Table 2. The C 1s core peaks corresponding to the contamination carbon are deconvoluted into three peaks: the main peak at 285.0 eV assigned to C—C or C—H bonds, the peak at 286.6 and 289.3 eV corresponding to C—O bonds and O=C—O bonds, respectively.

Due to spin-orbit coupling, the Ti 2p spectrum of each sample (Fig. 3) consist of two main Ti 2p components: Ti $2p_{3/2}$ (ca. 459.1 eV) and Ti $2p_{1/2}$ (ca. 464.9 eV). Beside two main components, Ti 2p spectrum also exhibits two distinct charge-transfer satellite peaks at 13 eV above the $2p_{3/2}$ and $2p_{1/2}$ peaks positions. The binding energy of these components is representative of the tetravalent Ti^{4+} cation in an oxygen environment [24–26]. When TiO_2 P25 was modified by TS method at increasing temperatures, the position shift of Ti 2p core peaks was negligible. No peak corresponding to Ti^{3+} was observed in the Ti $2p_{3/2}$ core level spectra. These results indicated that the TS process did not influence the chemical environment of Ti^{4+} cations.

As XPS Ti 2p spectra, the O 1s core peaks of all samples (Fig. 4) present rather the same characteristics. The O 1s core peaks were asymmetric, which could be deconvoluted into two components: a main component (O_I) at 530.4 eV attributed to O^{2-} anions of oxide lattice and a minor component (O_{II}) at 531.6 eV corresponding to oxygen atoms of hydroxyl groups on the oxide surface [25].

However, the quantitative calculations of peak areas indicated the modification of surface composition when TiO_2 P25 was modified by TS method from 500 °C (Table 3). The O_I/Ti atomic ratio of TiO_2 P25 sample (calculated from the area ratio of O 1s peak corresponding to lattice oxygen to the Ti 2p core peaks) was found to be 2.0. This ratio was identical to the stoichiometric O_I/Ti atomic ratio of TiO_2. For P25-500 sample, the O_I/Ti atomic ratio strongly decreased (O_I/Ti = 1.84), which suggests the deficiency of oxygen on the surface of this catalyst. At TS temperature of 700 °C and 950 °C, this ratio increased to 1.92 and 1.98, respectively. We also observed the same evolution of O_I/Ti atomic ratio for the TS-fluorinated

Table 1
Phase composition, crystal size and BET-surface area of TiO_2 P25, TS-modified catalysts and TS-fluorinated TiO_2.

Samples	Fraction (%)			BET surface area ($m^2\,g^{-1}$)
	Anatase (crystallite size (nm))	Rutile (crystallite size (nm))	$K_2Ti_6O_{13}$	
TiO_2 P25	89.8 ± 0.8 (21.6)	10.1 ± 0.3 (26.9)		34.837
P25-500	90.0 ± 1.5 (26.0)	10.0 ± 0.6 (25.7)		34.878
P25-700	86 ± 1 (30.6)	14.0 ± 0.5 (52.5)		26.642
P25-950		100 ± 3 (69.5)		
FTO-500 [13]	86 ± 2 (26.1)	13.9 ± 0.6 (29.5)		47.816
FTO-700 [13]	34.3 ± 0.9 (26.4)	17.1 ± 0.6 (36.3)	48.5 ± 0.5	
FTO-950 [13]		6.1 ± 0.2 (37.0)	93.8 ± 0.8	

Table 2
High resolution XPS data of TiO_2 P25 and modified catalysts by TS method.

	P25		P25-500		P25-700		P25-950	
	E_B (FWHM) (eV)	(%)	E_B (FWHM) (eV)	(%)	E_B (FWHM) (eV)	(%)	E_B (FWHM) (eV)	(%)
C 1s	285.0 (1.6)	5.60	285.0 (1.6)	6.12	285.0 (1.4)	14.62	285.0 (1.4)	5.65
	286.7 (1.6)	1.18	286.5 (1.6)	1.31	286.5 (1.6)	1.64	286.4 (1.6)	1.41
	289.4 (1.5)	0.82	289.5 (1.6)	0.82	289.2 (1.3)	0.99	289.3 (1.5)	0.98
Ti $2p_{3/2-1/2}$	459.1–464.9 (1.0-1.9) 472.3–478.2	28.80	459.3–465.0 (0.9-1.9) 471.7–478.6	30.21	458.9–464.6 (0.9–1.9) 471.6-478.0	26.66	459.1–464.8 (1.2–2.1) 471.5–478.4	28.18
Satellites	530.4 (1.1)	57.80	530.5 (1.1)	55.72	530.1 (1.1)	51.35	530.3 (1.1)	55.80
O 1s I	531.6 (1.5)	6.91	531.7 (1.6)	5.81	531.5 (1.6)	4.74	531.6 (1.6)	7.98
O 1s II	71.3	71.2	71.2	71.2				
ΔE_L (Ti 2p-O_I 1s) (eV)								

catalysts determined in [16]. In fact, for FTO-500, FTO-700 and FTO-950, the O_I/Ti atomic ratio was respectively 1.87, 1.93 and 1.99.

Moreover, O_{II}/Ti atomic ratio of catalyst surface was also influenced by TS process (Table 3). The O_{II}/Ti ratio of P25-700 sample slightly decreased in comparison with that of TiO_2 P25 and P25-500 samples. This ratio greatly increased at TS temperature of 950 °C. This seems to indicate that the complete formation of rutile phase due to high TS temperatures promotes the formation of surface hydroxyl groups. When TS process was combined with fluorination, the variation of surface hydroxyl group content became more complex. The FTO-500 catalyst showed a highest O_{II}/Ti atomic ratio of 0.31 while this ratio of P25-500 sample was almost identical to the naked TiO_2 P25 (O_{II}/Ti = 0.20). This difference demonstrated the fact that at 500 °C, an increase of surface's hydroxyl group amount can not be obtained by only the TS, but by the combination between the TS and surface fluorination of catalysts. However the content of surface hydroxyl groups dramatically decreased on FTO-700 and FTO-950 samples, which may results from the growth of oxide particles at high TS temperatures.

3.3. Optical properties

The UV–vis diffuse reflectance spectra of TiO_2 P25 and TS-modified catalysts were shown in Fig. 5. Compared with the optical absorption of TiO_2 P25, all TS-modified samples showed a red-shift of absorption edge toward longer wavelengths. This clearly indicates a decrease in the band gap energy of TiO_2. The E_g values of TiO_2 P25 and TS-modified catalysts were summarized in Table 3 in comparison with E_g of FTO catalysts determined in [16]. Surprisingly, when TiO_2 was modified by TS at 500 °C, the band gap energy greatly decreased from 3.64 eV (naked TiO_2 P25) to 3.45 eV (P25-500) although no change in phase composition was observed for this sample. This evolution was also observed for FTO-500 sample (E_g = 3.55 eV). When TS temperature increased up to 950 °C, the E_g value continued to decrease (3.10 eV for P25-950), which was attributed to the phase transition from anatase to rutile since the rutile phase posses a narrower band gap (~3.0 eV) [27] in comparison with anatase phase. However, in the case of TS-fluorinated catalysts, E_g value increased with TS temperatures. The rise of E_g in FTO-700 (E_g = 3.61 eV) and FTO-950 (E_g = 3.68 eV) should be attributed to the formation of $K_2Ti_6O_{13}$.

3.4. Adsorption of methylene blue

Fig. 6 compares the MB adsorption on catalysts used in this study and in [13–16]. At adsorption equilibrium, the adsorbed MB amount on the surface of TS-modified catalysts was only slightly superior to that on TiO_2 P25 whereas the TS-fluorinated catalysts clearly showed a higher MB adsorption capacity than TiO_2 P25. Among these catalysts, the FTO-500 exhibited the best MB adsorption (% adsorbed MB = 38.5%). It should be noted that the adsorption of MB on TiO_2 is driven by electrostatic interactions between MB molecules and functional groups on the surface of TiO_2. When TiO_2 P25 was fluorinated, the increase of BET surface area and the presence of strongly electronegative fluoride ions on the surface may induce a negative charge on the surface sample and then promoted the adsorption of organic cationic compounds such as MB. Moreover, the fluorination was also able to increase the amount of surface acid sites [28,29]. Owing to their strong electronegativity, the chemisorbed fluoride ions identified by XPS studies on the surface of fluorinated samples [16] can rise the positively charged of the neighbouring titanium atoms which can thus acting as Lewis acid sites. These sites could interact with the negatively charged π electrons of the aromatic compounds [29], such as

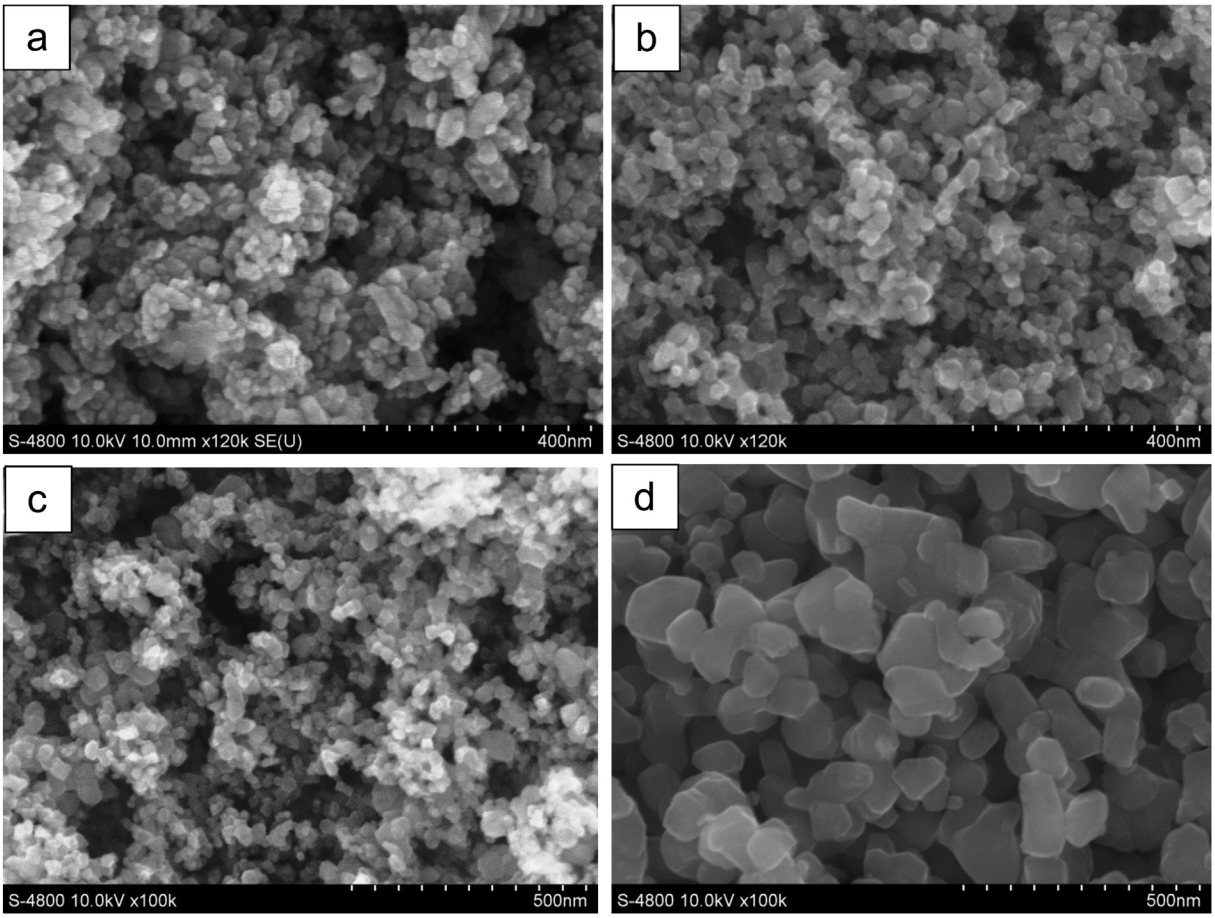

Fig. 2. SEM micrographs of (a) TiO_2 P25, (b) P25-500, (c) P25-700 and (d) P25-950.

MB and therefore further its adsorption. However, when TS temperature increased up to 950 °C, the MB adsorption on fluorinated samples dramatically decreased, according to the growth of particles which could decrease the specific surface of oxide. This is surprising that although SEM studies demonstrated the increase of particle size for P25-950 sample, this catalyst did not show a reduced MB adsorption, but a MB adsorption capacity comparable to TiO_2 P25 and TS-modified samples. This result could be explained by the great content of surface hydroxyl groups on the surface of PFTO-950. Dyes containing amin groups like MB can easily form hydrogen/electrostatic bonding with the surface hydroxyl group of catalysts. Thus the increase of surface OH groups on P25-950 may lead to the enhanced adsorption capacity.

3.5. Photocatalytic degradation of methylene blue under UV light

It should be noted that the mineralization of MB is always slower than its degradation, which has been proved by many studies [30–32]. There is the accumulation of intermediaries originated from the initial opening of the central aromatic rings of MB and their subsequent metabolites that retard the complete MB mineralization [30]. This observation is supported by the fact that during all photocatalytic reactions, the solution pH remains constant. In fact, different species such as NH_3, NH_4^+, H^+ [31] produced during the mineralization of MB can change the solution pH. If the mineralization and the degradation of MB have the same rate limiting step, a change in pH should have been observed. On the other hand, the

Table 3
Comparison of phase composition, surface features: $O_{lattice}$/Ti (O_I/Ti), O_{OH}/Ti (O_{II}/Ti), $F_{chemisorbed}$/Ti (F_{ads}/Ti) ratios from XPS data, band gap values (E_g) determined from UV–vis diffuse reflectance spectra and rate constant k of MB degradation on TiO_2 P25, TS-modified catalysts and TS-fluorinated catalysts.

		Samples						
		TiO_2 P25	P25-500	P25-700	P25-950	FTO-500 [13]	FTO-700 [13]	FTO-950 [13]
Phase composition	Anatase	89.8 ± 0.8	90.0 ± 1.5	86 ± 1		86 ± 2	34.3 ± 0.9	
	Rutile	10.1 ± 0.3	10.0 ± 0.6	14.0 ± 0.5	100 ± 3	13.9 ± 0.6	17.1 ± 0.6	6.1 ± 0.2
	$K_2Ti_6O_{13}$						48.5 ± 0.5	93.8 ± 0.8
Surface features	O_I/Ti	2.00	1.84	1.93	1.98	1.87	1.93	1.99
	O_{II}/Ti	0.20	0.19	0.17	0.28	0.31	0.26	0.21
	F_{ads}/Ti					0.13	0.16	0.25
E_g (eV)	3.64	3.45	3.43	3.10	3.55	3.61	3.68	
K	5034.7	6427.3	5171.8	5009.4	7491.9	8576.3	5660.9	
k_{app} (h^{-1})	Under UV light	1.46	1.82	1.60	0.52	2.09	1.56	0.47
	Under visible light	0.20	0.28	0.29	0.34	0.32	0.20	0.07

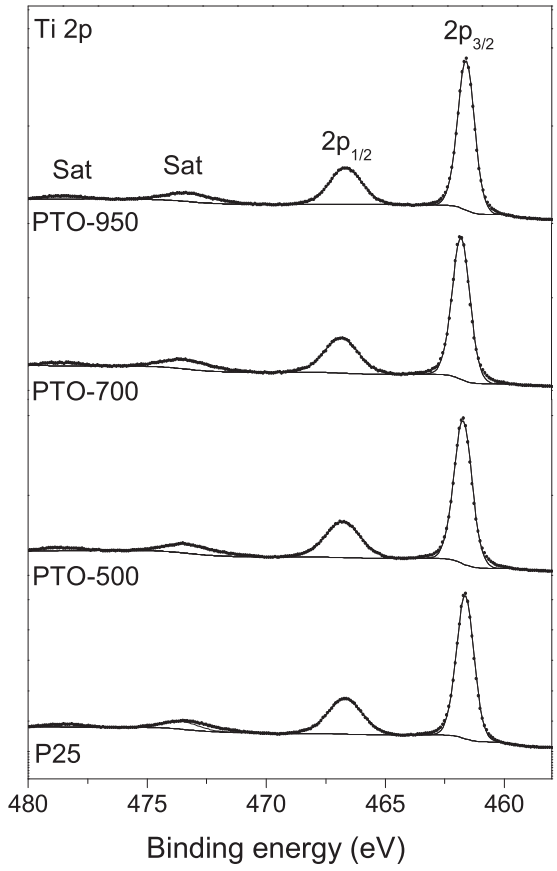

Fig. 3. Ti 2p spectra of TiO_2 P25 and modified samples by TS method.

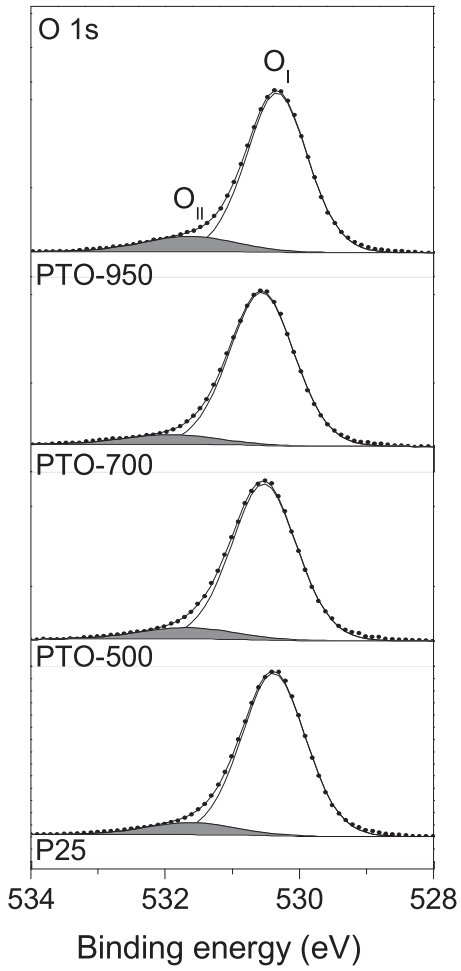

Fig. 4. O 1s spectra of TiO_2 P25 and modified samples by TS method.

MB mineralization is usually evaluated by measuring the chemical oxygen demand of its solution. In general, the photocatalysis was applied for the oxidation of organic pollutants in low concentrations. Thus, in our study, we chose the initial MB concentration of 10^{-5} mol L^{-1}. The measurement of chemical oxygen demand of MB solution before and after photocatalytic treatment is inappropriate with this low concentration since this method often shows significant errors. Therefore, we only followed the degradation of MB in this work, in order to compare the photocatalytic activity of oxide samples.

Fig. 7 shows a comparison of Ln (C_0/C) curves of MB degradation on different samples under UV irradiation (C is the MB concentration at time t and C_0 is the initial MB concentration). It was found that the net decomposition of MB in the aqueous solution followed the pseudo-first-order Langmuir–Hinshelwood kinetic model, according to the expression:

$$r = kK\frac{[\mathrm{MB}]}{1+K[\mathrm{MB}]} = k_{\mathrm{obs}}[\mathrm{MB}]$$

where r is the reaction rate of MB degradation, k is the rate at maximum catalyst coverage, K is the adsorption coefficient of MB and k_{obs} is the observed pseudo-first-order rate constant.

Table 3 summarized the k_{obs} and K values of all catalysts. Since [MB] = 10^{-5} mol L^{-1}, it was found that all K[MB] values are very inferior to 1, which means that the k_{obs} can be considered as a constant for each catalyst. Therefore, the evaluation of photocatalytic activity relies on the comparison of MB degradation rate constant (k_{obs}). Under UV irradiation, the rate constant of MB degradation on TiO_2 P25 sample reached 1.46 h^{-1}. After the TS process at 500 °C, the photocatalytic activity strongly increased (k_{obs} = 1.81 h^{-1}). More specially, the combination between TS and fluorination further increased the photocatalytic performance. The best UV-light-induced photocatalyst was FTO-500 with k_{obs} = 2.09 h^{-1}.

However, for the TS process above 700 °C, the activity of all photocatalysts decreased with TS temperatures. In the case of TS-modified catalysts, the rate constant of MB degradation was k_{obs} = 1.60 and 0.52 h^{-1} for P25-700 and P25-950, respectively. For the FTO samples, the decrease of photocatalytic activity was

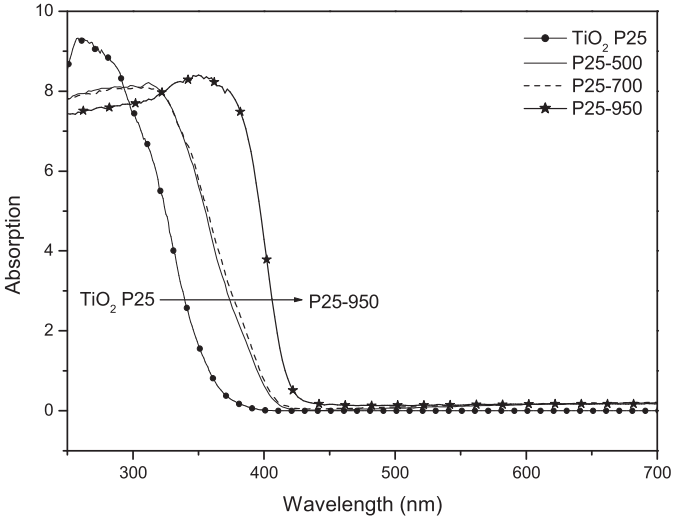

Fig. 5. UV–visible diffuse reflectance spectra of TiO_2 P25 and TS-modified catalysts.

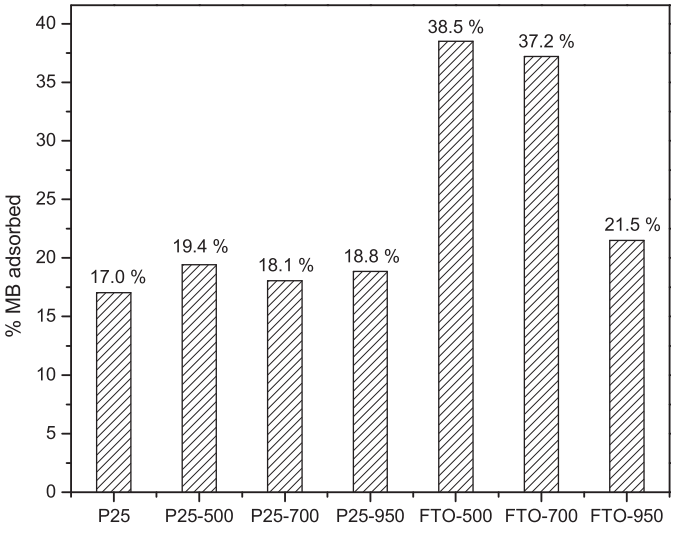

Fig. 6. Comparison of MB amount adsorbed on the surface of samples.

also clearly observed on FTO-700 ($k_{obs} = 1.56\,h^{-1}$) and FTO-950 ($k_{obs} = 0.47\,h^{-1}$).

3.6. Photocatalytic degradation of methylene blue under visible light

Fig. 8 compares the Ln (C_0/C) curves of MB degradation on different samples under visible irradiation. Similar to the MB degradation under UV irradiation, this phenomenon under visible light followed the pseudo-first-order Langmuir–Hinshelwood kinetic model. The rate constant of MB degradation on photocatalysts was presented in Table 3. The TiO_2 P25 sample presented $k_{obs} = 0.20\,h^{-1}$ whereas the P25-500 catalyst showed $k_{obs} = 0.28\,h^{-1}$. We also observed a slightly increased of rate constant of MB degradation on P25-700 sample ($k_{obs} = 0.29\,h^{-1}$). More especially, at TS temperature of 900 °C, this rate constant greatly increased ($k_{obs} = 0.34\,h^{-1}$, 1.7 times higher than TiO_2 P25). These results proved that our TS method does not only improve the UV light induced photocatalysis but also increase the photocatalytic activity under visible illumination.

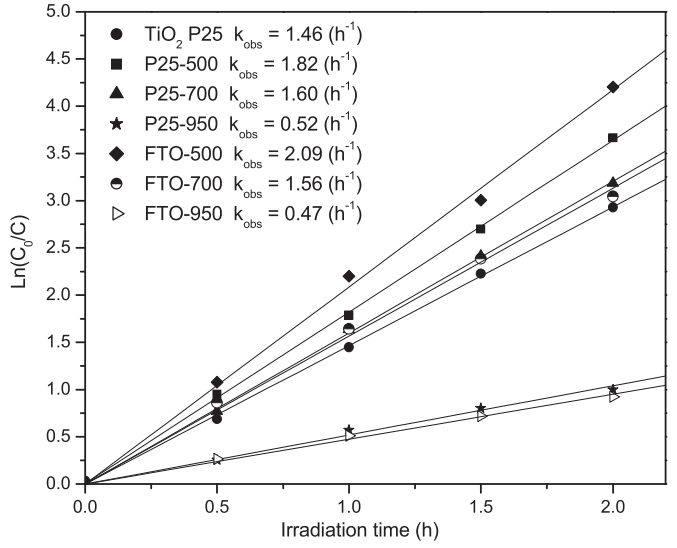

Fig. 7. Ln(C_0/C) versus time plot for determination of rate constants k_{obs} (h^{-1}) of MB degradation under UV irradiation.

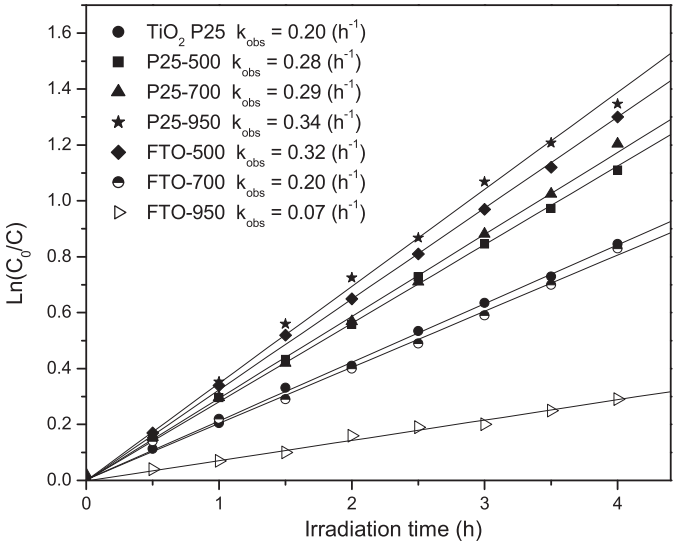

Fig. 8. Ln(C_0/C) versus time plot for determination of rate constants k_{obs} (h^{-1}) of MB degradation under visible irradiation.

It should be noted that our previous study [16] revealed a different evolution of rate constants of MB degradation on TS-fluorinated catalysts under visible light. The fluorination by TS method also improved the photocatalytic activity under visible light. The FTO-500 sample showed the best performance with $k_{obs} = 0.32\,h^{-1}$ (1.6 times higher than TiO_2 P25). However, when the fluorination occurred at higher TS temperatures such as 700 and 900 °C, the rate constant decreased to $k_{obs} = 0.20\,h^{-1}$ and $0.07\,h^{-1}$, respectively.

4. Discussion

In our work, the TS method was used to modify the properties of TiO_2. The results of characterization study and photocatalytic tests showed that the effects of TS strongly depend on the TS temperatures. In fact, it was observed that the TS process at 500 °C did not modify the crystal structure, the morphology, even the surface hydroxyl groups of the oxide. It should be noted that the adsorption of MB on P25-500 was slightly higher than TiO_2 P25. However, the activity of P25-500 was greatly superior to that of TiO_2 P25 under both UV and visible light illumination. This could only be explained by the formation of surface defects on P25-500 catalyst. According to the XPS results, the O_I/Ti atomic ratio strongly decreased from 2, the stoichiometric O/Ti ratio for TiO_2 P25 to 1.84 for P25-500. The reduced O/Ti ratio of this catalyst should be attributed to the deficiency of oxygen on the surface due to the TS process. Nevertheless, we did not observe the presence of Ti^{3+} on the surface by XPS experiments. Thus, the origin of surface oxygen deficiency may be very complicated, which can not be only elucidated by the indirect evidence of surface O/Ti ratios in our work and thus needs to be further studied. However, the surface O/Ti ratio is still the important factor which contributes in the relationship between surface defects and photocatalytic activity. From this viewpoint, we suggest that one of the reasons for the oxygen deficiency may be the formation of surface oxygen vacancies. In fact, some studies in literature [12,33] also assigned the oxygen deficiency detected by XPS to the surface oxygen vacancies.

It has been reported that the surface oxygen vacancies could create two types of shallow trap in the electronic structure of TiO_2: one color center with two trapped electrons and the other with one trapped electron. Their electronic state is respectively located at 0.5 and 0.8 eV below the conduction band [3,4,34], which can

lead to the narrowing of band gap. Therefore, when TiO_2 P25 was modified by TS method at 500 °C in our work, the reduction of band gap may be related to the formation of surface oxygen vacancies. As a result, this effect can enhance the probability of electron transition from the valence band to the condution band and reduce the required energy for the photoexcitation. Moreover, the oxygen deficient sites on the catalyst surface were found to play as electron trapping centers which can effectively capture the photoinduced electrons and inhibit the recombination of photoinduced electrons and holes [12,31,35]. This would assure a sufficiently long lifetime of photoinduced holes and thus promote the generation of OH• radicals, which play a key role in the oxidation of organic substrates.

More specially, when the fluorination was combined with TS at 500 °C, the photocatalytic activity of TiO_2 was further improved under UV and visible light illumination. As described in [16], the fluorination by TS at 500 °C did not only form the surface defects but also increased the surface hydroxyl group content of TiO_2 (Table 3). According to the mechanism of OH• radical formation, most of OH• radicals are formed from the reaction of photogenerated holes and surface OH groups [36,37]. Thus, the increase of surface OH groups enhanced the content of OH• radicals, resulting in the improved photocatalytic activity. Moreover, the presence of fluoride ions on the surface of fluorinated TiO_2 was suggested to generate two effects. Firstly, the chemisorbed F^- ions may induce the energetic levels in the electronic structure of TiO_2, which facilitates the photoexcitation of electrons in the valence band. Secondly, owing to its strongly electronegative, fluoride ions can captured the photogenerated electrons and then increased the hole availability of TiO_2 [38,39], which also allows holes to react with surface OH groups to produce more OH• radicals for the oxidation of organic pollutants.

However, when TS was carried out at 700 and 950 °C, the evolution of photocatalytic activity became more complex. Under UV light, the rate constant of MB degradation on P25-700 and P25-950 decreased to 1.60 and 0.52 h^{-1} (compared to 1.82 h^{-1} for P25-500), respectively. Interestingly, although the P25-950 catalyst showed the highest content of surface OH groups, the rate constant of MB degradation on this oxide was the lowest value. This could be explained by the complete phase transition from anatase to rutile which often presents the lower photocatalytic properties than anatase [23] and by the strong growth of catalyst particles at 950 °C which could decline the specific surface and then the number of reactive sites on the surface of catalyst. Conversely, under visible light, the activity of these samples was superior to P25-500 and TiO_2 P25. Their enhanced visible-light-induced photocatalytic activity is in good agreement with the result of XRD study. From TS temperature of 700 °C, XRD patterns showed the increase of rutile phase in TiO_2, which led to the declined band gap energy of TS-modified catalyst as presented in their UV–visible diffuse reflectance spectra. Thus, rutile phase could operate under visible light illumination. As a result, when the rutile amount increases, the visible-light-driven performance of catalysts is improved.

Different from the case of TS-modified catalysts, the photocatalytic performance of fluorinated catalysts decreased under both UV and visible light illumination when the fluorination TS temperature reached 700 and 950 °C. The declined performance can be explained by the formation of $K_2Ti_6O_{13}$ and the particle growth. It was reported that $K_2Ti_6O_{13}$ presents a lower activity than TiO_2 P25 [40]. On the other hand, the increase of particle size for these samples observed by SEM studies in [16] might lead to the reduction of their specific surface area, which could decrease the amount of surface OH groups, hinder the MB adsorption and limit the diffusion of photoexcited electron-hole pairs on the surface, resulting in the reduction of photocatalytic activity.

5. Conclusion

In this work, we studied the influences of thermal shock method at different temperatures on the crystal structure, morphology, surface composition and photocatalytic activity of TiO_2 P25. The properties of TS-modified catalysts were also compared with TS-fluorinated TiO_2 in our previous study in order to elucidate the synergic effects of thermal shock and fluorination process. The results indicated that the TS without fluorination and with fluorination were strongly depending on TS temperatures. At low temperature (500 °C), the TS method without fluorination did not modify the phase composition, particle size of this oxide but created the deficiency of oxygen on the surface of catalysts, which led to the red shift of absorption edge and promoted the MB photodegradation under UV and visible light illumination. Therefore, by TS method, a simple and quick method, we have successfully prepared new highly photocatalytic materials. When the thermal shock was combined with fluorination, the simultaneous presence of surface oxygen deficiency, chemisorbed fluoride ions and the enhanced surface hydroxyl groups greatly improved the photocatalytic performance. However, at higher temperatures, for the TS without fluorination, the phase transition from anatase to rutile only enhanced the photocatalytic activity under visible light, not under UV light. For the fluorinated catalysts, the TS at high temperatures induced the formation of $K_2Ti_6O_{13}$ and the growth of particles which declined the activity under both UV and visible light.

Acknowledgment

This work was supported by the National Foundation for Science and Technology Development of Vietnam (NAFOSTED, Project no. 104.02-2012.53).

References

[1] A.L. Linsebigler, G. Lu, J.T. Yates, Chem. Rev. 95 (1995) 735.
[2] D. Li, N. Ohashi, S. Hishita, T. Kolodiazhnyi, H. Haneda, J. Solid State Chem. 178 (2005) 3293.
[3] D. Li, H. Haneda, N.K. Labhsetwar, S. Hishita, N. Ohashi, Chem. Phys. Lett. 401 (2005) 579.
[4] W. Ho, J.C. Yu, S. Lee, Chem. Commun. 10 (2006) 1115.
[5] T.R. Gordon, M. Cargnello, T. Paik, F. Mangolini, R.T. Weber, P. Fornasiero, C.B. Murray, J. Am. Chem. Soc. 134 (2012) 6751.
[6] J. Wang, D.N. Tafen, J.P. Lewis, Z. Hong, A. Manivannan, M. Zhi, M. Li, N. Wu, J. Am. Chem. Soc. 131 (2009) 12290.
[7] B.J. Morgan, G.W. Watson, Phys. Rev. B 80 (2009) 233102.
[8] X. Pan, N. Zhang, X. Fu, Y.-J. Xu, Appl. Catal. A 453 (2013) 181.
[9] T. Torimoto, R.J. Fox, M.A. Fox, J. Electrochem. Soc. 143 (1996) 3712.
[10] A.-K. Axelsson, L.J. Dunne, J. Photochem. Photobiol. A: Chem. 144 (2001) 205.
[11] J.C. Wang, P. Liu, X.Z. Fu, Z.H. Li, W. Han, X.X. Wang, Langmuir 25 (2009) 1218.
[12] T. Ihara, M. Miyoshi, Y. Iriyama, O. Matsumoto, S. Sugihara, Appl. Cat. B: Environ. 42 (2003) 403.
[13] W. Kongsuebchart, P. Praserthdam, J. Panpranot, A. Sirisuk, P. Supphasrirongjaroen, C. Satayaprasert, J. Cryst. Growth 297 (2006) 234.
[14] Q. Xiao, Z. Si, Z. Yu, G. Qiu, Mater. Sci. Eng. B 137 (2007) 189.
[15] X. Pan, M.-Q. Yang, X. Fu, N. Zhang, Y.-J. Xu, Nanoscale 5 (2013) 3601.
[16] T.K. Le, D. Flahaut, D. Foix, S. Blanc, H.K.H. Nguyen, T.K.X. Huynh, H. Martinez, J. Solid State Chem. 187 (2012) 300.
[17] T.K. Le, D. Flahaut, H. Martinez, T. Pigot, H.K.H. Nguyen, T.K.X. Huynh, Appl. Catal. B: Environ. 144 (2014) 1.
[18] R.G. Nair, S. Paul, S.K. Samdarshi, Sol. Energy Mater. Sol. C 95 (2011) 1901.
[19] J. Rodriguez-Carvajal, IUCr Newslett. 26 (2001) 12.
[20] D.A. Shirley, Phys. Rev. B 5 (1972) 4709.
[21] J.H. Scofield, J. Electron Spectrosc. Relat. Phenom. 8 (1976) 129.
[22] A.B. Murphy, Appl. Opt. 46 (2007) 3133.
[23] R.G. Nair, S. Paul, S.K. Samdarshi, Sol. Energy Mater. Sol. C 95 (2011) 1901.
[24] M.G. Faba, D. Gonbeau, G. Pfister-Guillouzo, J. Electron Spectrosc. Relat. Phenom. 73 (1995) 65.
[25] J.C. Dupin, D. Gonbeau, P. Vinatier, A. Levasseur, Phys. Chem. Chem. Phys. 2 (2000) 1319.
[26] C. Guimon, A. Gervasini, A. Auroux, J. Phys. Chem. B 105 (2001) 10316.
[27] J. Pascual, J. Camassel, H. Mathieu, Phys. Rev. Lett. 39 (1977) 1490.
[28] D. Li, H. Haneda, S. Hishita, N. Ohashi, N.K. Labhsetwar, J. Fluor. Chem. 126 (2005) 69.

[29] D.G. Huang, S.-J. Liao, J.-M. Liu, Z. Dang, L. Petrik, J. Photochem. Photobiol. A 184 (2006) 282.
[30] A. Houas, H. Lachheba, M. Ksibi, E. Elaloui, C. Guillard, J.-M. Herrmann, Appl. Catal. B 31 (2001) 145.
[31] H. Lachheb, E. Puzenat, A. Houas, M. Ksibi, E. Elaloui, C. Guillard, J.M. Herrmann, Appl. Catal. B 39 (2002) 75.
[32] H. Huang, D.Y.C. Leung, P.C.W. Kwong, J. Xiong, L. Zhang, Catal. Today 201 (2013) 189.
[33] T. Ihara, M. Miyoshi, M. Ando, S. Sugihara, Y. Iriyama, J. Mater. Sci. 36 (2001) 4201.
[34] D.-R. Park, J. Zhang, K. Ikenue, H. Yanashita, M. Anpo, J. Catal. 185 (1999) 114.
[35] B. Xin, D. Ding, Y. Gao, X. Jin, H. Fu, P. Wang, Appl. Surf. Sci. 255 (2009) 5896.
[36] C. Minero, G. Mariella, V. Maurino, E. Pelizzetti, Langmuir 16 (2000) 8964.
[37] C. Minero, G. Mariella, V. Maurino, E. Pelizzetti, Langmuir 16 (2000) 2632.
[38] S.Y. Yang, Y.Y. Chen, J.G. Zheng, Y.J. Cui, J. Environ. Sci. 19 (2007) 86.
[39] C. Yu, J.C. Yu, M. Chan, J. Solid State Chem. 182 (2009) 1061.
[40] F. Amano, T. Yasumoto, T. Shibayama, S. Uchida, B. Ohtani, Appl. Catal. B: Environ. 89 (2009) 583.